Chapter 3

Enhanced Permeability and Retention (EPR) Effect for Anticancer Nanomedicine Drug Targeting

Khaled Greish

Abstract

Effective cancer therapy remains one of the most challenging tasks to the scientific community, with little advancement on overall cancer survival landscape during the last two decades. A major limitation inherent to most conventional anticancer chemotherapeutic agents is their lack of tumor selectivity. One way to achieve selective drug targeting to solid tumors is to exploit abnormalities of tumor vasculature, namely hypervascularization, aberrant vascular architecture, extensive production of vascular permeability factors stimulating extravasation within tumor tissues, and lack of lymphatic drainage. Due to their large size, nano-sized macromolecular anticancer drugs administered intravenously (i.v.) escape renal clearance. Being unable to penetrate through tight endothelial junctions of normal blood vessels, their concentration builds up in the plasma rendering them long plasma half-life. More importantly, they can selectively extravasate in tumor tissues due to its abnormal vascular nature. Overtime the tumor concentration will build up reaching several folds higher than that of the plasma due to lack of efficient lymphatic drainage in solid tumor, an ideal application for EPR-based selective anticancer nanotherapy. Indeed, this selective high local concentration of nano-sized anticancer drugs in tumor tissues has proven superior in therapeutic effect with minimal side effects in both preclinical and clinical settings.

Key words: EPR effect, nanomedicines, half-life, targeted anticancer therapy, macromolecular drugs, tumor model, in vivo, biodistribution.

1. Introduction

Anticancer chemotherapy is one of the most notorious drugs known to human. The sole purpose of their use is cell killing, a task that usually achieved with high efficacy but little precision. Most anticancer chemotherapeutic agents used in clinic target dividing cells, regardless of its nature whether a dividing tumor cell or active intestinal epithelial cells, with same potency. The

S.R. Grobmyer, B.M. Moudgil (eds.), *Cancer Nanotechnology*, Methods in Molecular Biology 624,
DOI 10.1007/978-1-60761-609-2_3,

term of maximum tolerated dose thus is not based on the amount needed to cure the disease, conversely on the amount needed not to incapacitate the host. Alternatively, anticancer targeting proved to be a more effective approach with minimum toxicity. On the gross level, tumor vasculature proved to be a potential target for cancer treatment. Tumor vascular typically comprised of poorly aligned defective endothelial cells with wide fenestrations (up to 4 μm), lacking smooth muscle layer or innervations, with relatively wide lumen and impaired receptor function for vasoactive mediators especially angiotensin II; further they lack functional lymphatics (1–5). In addition, hyperproduction of vascular mediators, such as vascular endothelial growth factor, bradykinin, nitric oxide peroxynitrite, prostaglandins, and matrix metalloproteinases (6–10), contributes greatly to this hyperpermeability in tumor tissues. EPR effect involves two major components, first altered biodistribution, where the nano-size drug shows differential accumulation in the tumor tissues reaching higher concentration than that in the plasma or other organs (**Fig. 3.1A**), this effect is time dependent and can be reproduced in tumors of different size as shown in **Fig. 3.1B**. EPR effect is mainly the function of molecular weight with molecules ranging 40–800 kD can exhibit preferential tumor targeting (**Fig. 3.1C**).

The other aspect of EPR effect is increased plasma half-life of the nano-size drugs as their size exceeded the limit of renal excretion threshold, limiting their clearance (**Fig. 3.1D**). As pharmacological effect and plasma concentration are parallel, this phenomenon results in prolonged therapeutic effect in addition to targeting (11, 12). The gain expected from EPR effect is in the magnitude of 7- to 10-fold higher tumor concentration compared to equivalent doses of the same drug at low molecular weight form (13). EPR is a passive phenomenon that can be actively augmented by the following techniques related to the abnormalities of tumor vasculature.

1.1. Hypertension

In normal blood vessels, the smooth muscle layer responds to vascular mediators such as bradykinin, acetylcholine, NO, and calcium via the receptors on smooth muscle cells of blood vessels, and hence helps maintain constant blood flow volume (**Fig. 3.2 a B**). Raising the systolic blood pressure from 100 to 150 mm Hg for 15 min by infusing angiotensin II (AT II) into tumor-bearing rats caused 2- to 6-fold selective increase in tumor blood flow; blood flow in normal organs and tissues remained constant regardless of the induced blood pressure (14). When ^{51}Cr-labeled-SMANCS or ^{51}Cr-albumin was injected i.v. under AT-II-induced hypertension, 3-fold higher accumulation was achieved in tumor tissue compared to normotensive condition. Additionally, the amount of drug delivered to normal organs such as kidney and bone marrow was reduced because of the

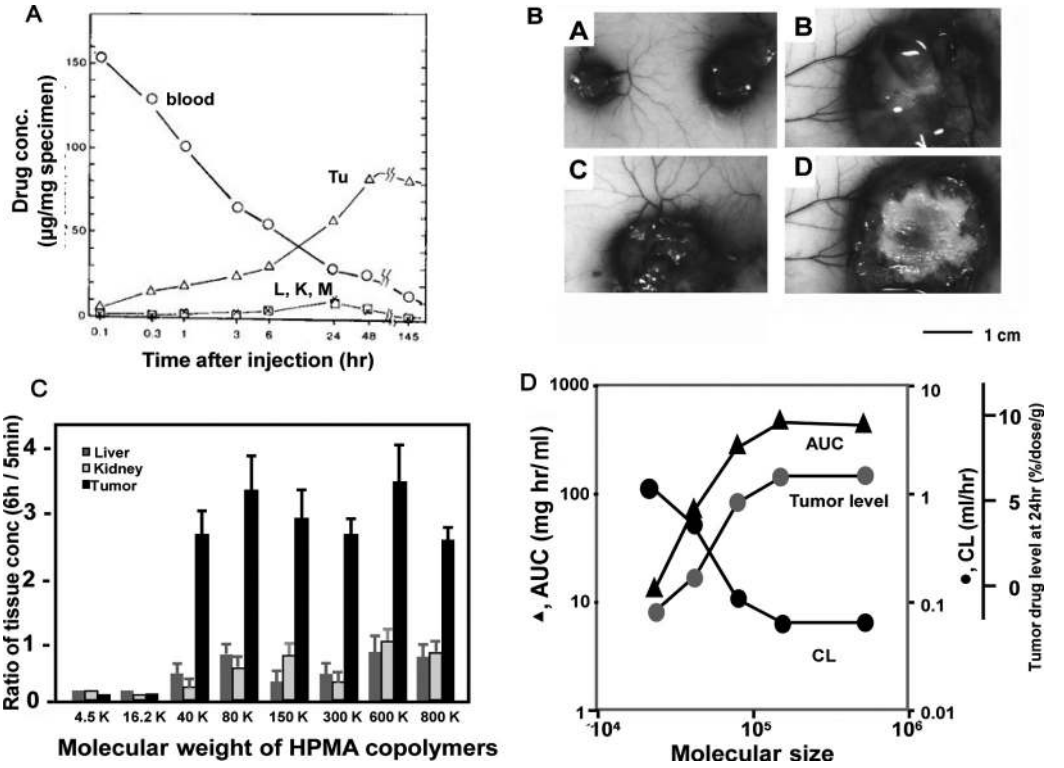

Fig. 3.1. Selective accumulation of Evans blue dye bound to albumin (70 kDa) in S 180 tumor in DdY mice. **a**, Blood concentration versus tumor, liver, kidney, and muscle. The graph represents the result of methods in **Section 3.2**. **b**, EBD accumulation in small tumor (*A*), large tumor (*B*), (*C*) shows the retention of the dye at 24 h and (*D*) is cross section of (*B*), the central region of the tumor is necrotic and avascular, and hence does not facilitate the uptake of nano-size EBD. **c**, The accumulation of ^{125}I-labeled *N*-(2-hydroxypropyl) methacrylamide (HPMA) copolymer in the solid tumor tissues. Note that large macromolecules, but not smaller ones, manifest progressive accumulation. **d**, The relation between molecular weight, AUC, tumor accumulation, and renal clearance. (Reproduced from 27 with permission from Imperial College Press.)

vasoconstriction occurring in normal organs under AT-II-induced hypertension. However, mitomycin C (334.3 Da) did not produce the same effect under the same experimental conditions (15). Better therapeutic effect could be demonstrated in the clinical setting, by using this method with SMANCS/Lipiodol for tumors such as cholangiocarcinoma, metastatic liver cancer, and renal cancer (16).

1.2. Bradykinin (BK)

BK-generating cascade is normally activated in tumor tissues and was found to be involved in accumulation of malignant ascitic and pleural fluids in cancer patients. Various human and rodent solid tumors express excessive levels of BK receptor B2 (7–9). BK is degraded by many peptidases, especially angiotensin-converting enzyme (ACE). Therefore, ACE inhibitors can cause local increase of BK levels at the tumor site. On the basis of these data, we used the ACE inhibitors enalapril and temocapril

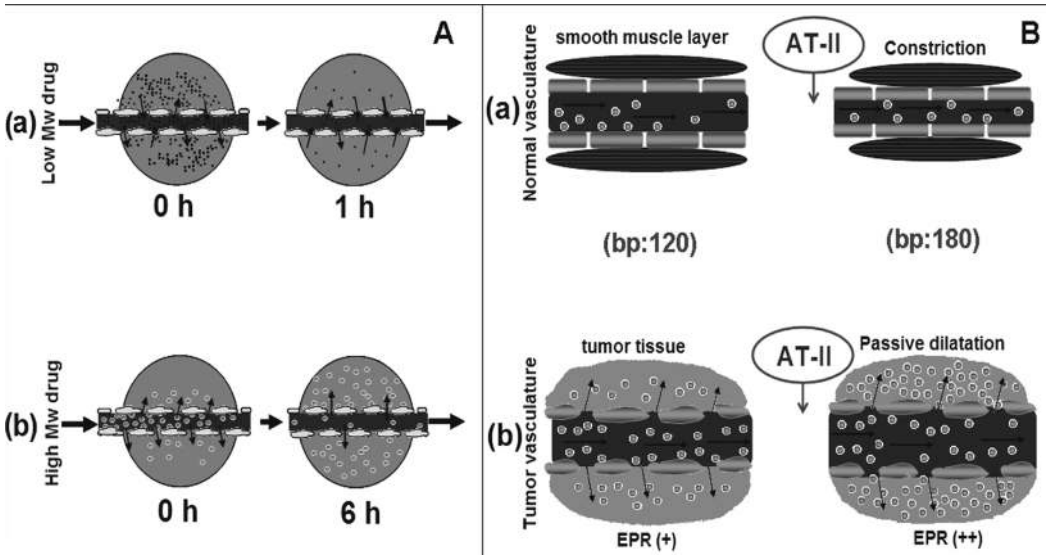

Fig. 3.2. Diagrammatic representation of EPR effect. (**A**) Shows the diffusion of a low molecular weight (*a*) and high molecular weight drug (*b*). Note progressive accumulation of macromolecular drug in the tumor tissues with time by the EPR effect. (**B**) Vascular leakage in relation to AT-II. Note that under AT-II-induced hypertensive state (**B**-*a*), vasoconstriction in the normal blood vessels occurs due to the presence of smooth muscle layer, while tumor vessels (**B**-*b*), passively dilate due to the absence of smooth muscle layer leading to enhanced extravasations of macromolecular drugs and hence augmentation of EPR effect. (Reproduced from 26 with permission from Elsevier.)

to inhibit BK degradation, this resulted in elevated BK level and further enhancement of the EPR effect (17). ACE inhibitors thus increase delivery of macromolecular drugs to tumors, even under normotensive conditions (**Fig. 3.3**).

1.3. Nitric Oxide (NO)

NO plays a key role in angiogenesis, cell proliferation, and EPR effect. NO is synthesized by NO synthase (NOS) from L-arginine. Consequently, inhibition of NO generation by NOS inhibitors as *N*-monomethyl-L-arginine was found to suppress tumor growth (7, 8, 10). NOS inhibitor irreversibly attenuated blood flow in R3230Ac rat mammary adenocarcinoma (18). In addition, we found that pro-matrix metalloproteinases (proMMPs) are activated by peroxynitrite (ONOO–), which is produced extensively in tumor and inflammatory tissues (19). Clinically, we have utilized the vasodilator effect of NO to increase the delivery of the nanomedicine drug SMANCS to tumor site in hepatocellular carcinoma by local injection of isosorbide dinitrate (ISDN) into the tumor-feeding artery (**Fig. 3.4**).

1.4. Photodynamic Therapy (PDT)

When a photosensitizer is administrated systemically or locally and subsequently activated by illumination with visible light, this leads to the generation of reactive oxygen species. This effect has active role in enhancing tumor vascular permeability (20, 21). The concentration of nano-size FITC-dextran was 5-fold higher

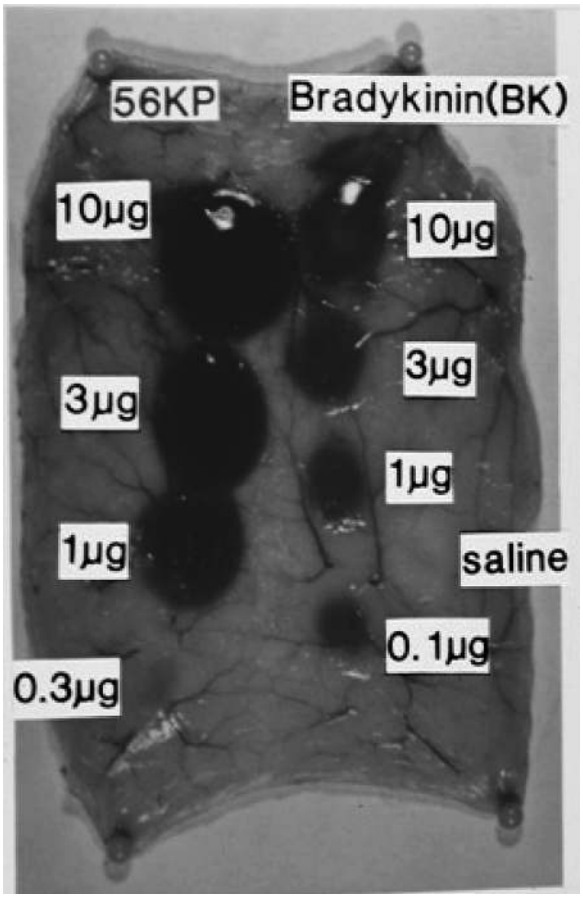

Fig. 3.3. Enhancement of permeability in the skin of guinea pig after SC injection of various doses of BK and the 56 kDa protease which induces kallikrein–kinin system. EBD was injected intravenously after 10 min of SC injection. The results show the enhancement of permeability at 6 h after injection of EBD.

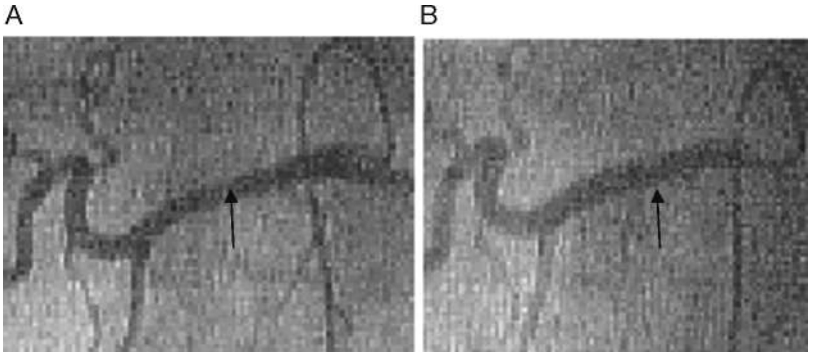

Fig. 3.4. The effect of local injection of the vasodilator isosorbide dinitrate (ISDN) on the diameter of the proper hepatic artery (*arrow*): (**a**) before ISDN and (**b**) after ISDN injection. Note the 187% increase in the vessel diameter (**b**), this technique was successfully used in the clinic to enhance SMANCS targeting into hepatic tumors.

in orthotropic MatLyLu rat prostate tumors treated with the photosensitizer verteporfin, at 15 min following light irradiation, compared to nonirradiated control group (21). Photosensitization causes endothelial cell microtubule depolymerization and induces the formation of actin stress fibers. Thus, endothelial cells were found to retract, leading to the formation of intercellular gaps, which result in enhanced vascular permeability. In addition, endothelial cell damage leads to the establishment of thrombogenic sites within the vessel lumen, and this initiates a physiological cascade of responses including platelet aggregation, the release of vasoactive molecules, leukocyte adhesion, and increases in vascular permeability (20). We have used the photosensitizer ZnPP to enhance tumor permeability and could achieve 3-fold higher accumulation of the Evans blue dye in tumor tissue after 5 min irradiation with ambient light (**Fig. 3.5**).

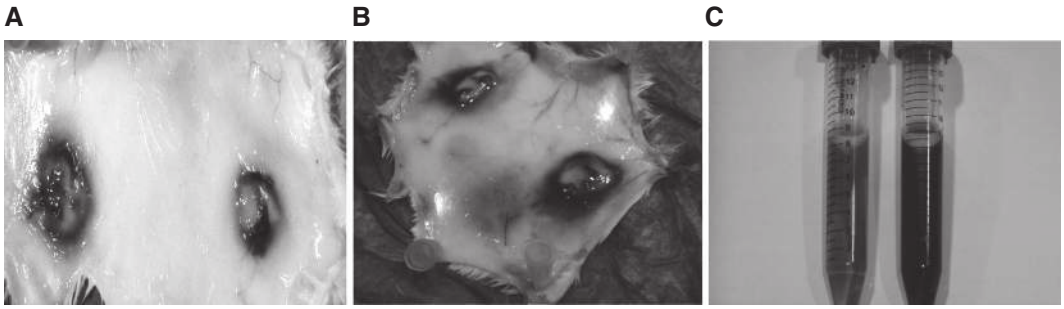

Fig. 3.5. Enhancement of the EPR effect by photodynamic therapy (PDT). (**a**), EBD concentration in S-180 murine sarcoma without PDT. (**b**) 15 min after injection of 5 mg/kg ZnPP photosensitizer, animals were injected with EBD 10 mg/kg. After another 30 min of ZnPP injection, animals were irradiated for 5 min at 50.000 Lux, 4 h after irradiation animals were scarified and EBD was quantified. (**c**), ZnPP-mediated photoactivity enhanced the EPR effect by 3-fold magnitude.

2. Materials

2.1. Establishment of In Vivo Tumor Model

1. Mouse sarcoma S-180 cells, ATCC Number TIB-66 (Manassas, VA).
2. Male DdY mice, 6 weeks old weighing 30–35 g (SLC, Inc., Shizuoka, Japan).
3. Isoflurane (MWI Veterinary Supply, MERIDIAN, ID).
4. Isoflurane vaporizer system (V3000PK, Parkland Scientific, Coral Springs, FL).

2.2. Demonstration of EPR Effect in Tumor Model

1. Evans blue dye (EBD) (Sigma Chemical Co., St. Louis, MO).
2. Formamide reagent grade, 98% (Sigma Chemical Co., St. Louis, MO).
3. Isoton II (Coulter Corporation, Miami, FL).

2.3. Styrene Maleic Acid (SMA) – Micelle Preparation

1. SMA (Kuraray Ltd., Kurashiki, Japan).
2. 1-Ethyl-3-(3-dimethylaminopropyl) carbodiimide (EDAC) (Dojindo, Kumamoto, Japan).
3. Doxorubicin (Sigma Chemical Co., St. Louis, MO).
4. Amicon ultrafiltration system (YM-10 membrane; cut-off molecular size of 10 kDa) (Millipore, Bedford, MA).

2.4. Pharmacokinetics of Nano-sized Micelle of Doxorubicin Versus Free Drug

1. ^{14}C Doxorubicin hydrochloride, 91.9% radio chemically pure with a specific radioactivity of 3.5 MBq/mg (Amersham, Buckinghamshire, UK).
2. Soluene-350 (Packard Instruments, Groningen, the Netherlands).
3. Hionic Fluor LSC cocktail (Packard Instruments, Meriden, CT).
4. Beta liquid scintillation counters (LSC-5100, Aloka, Tokyo, Japan).

3. Methods

3.1. Establishment of In Vivo Tumor Model

1. Inject 5×10^6 S-180 cells in 1 mL PBS into the right lower quadrant of the abdomen of DdY mice using 27-G needle.
2. Observe animals for 7–10 days, this is a proper time to aspirate the resulting ascetic fluid of tumor; longer time will result in bloody aspirate.
3. Euthanize animal using CO_2 for 2 min.
4. Place the animal on its side and insert G18 needle mounted 10 mL syringe into the most gravity-dependent point and aspirate cells.
5. Cells to be diluted with five times cold sterile PBS and centrifuged at 800 rpm at 4°C for 5 min to remove proteins and blood from cancer cells, repeat for two times or until the cell precipitates become clear.
6. Repeat Steps 1–5 for another extra passage before inducing SC tumor to insure high tumorgenic ability of cells.
7. Count a small sample of cell (5 μL) using trypan blue dye in hemocytometer.
8. Prepare 2×10^6 cells per 200 μL PBS and keep in ice.
9. Anesthetize animals using 3–4% isoflurane for 2–3 min in induction chamber of the vapor anesthesia system, then move animals to warm heated blanket, and use nose cone for anesthesia.

10. Shave two bilateral dorsal sites where tumor injection is intended.
11. Lay anesthetized animal ventrally, raise a dorsal skin fold with a tweezers, clean it with gauze soaked in 70% ethanol, and at near horizontal angel, insert the 27 G needle mounted on 1-mL syringe, inject cell slowly to prevent leakage from injection site. The development of SC bleb indicates successful injection.
12. Follow the animal daily for 7–10 days, at this time usually animal will develop tumors of 5–7 mm diameter which are optimal for EPR-related studies.

3.2. Demonstration of EPR Effect in Tumor Tissues

1. Dissolve Evans blue dye (EBD) in DW at final concentrations of 1 mg/mL, and then adjust the concentration to give final dose of 10 mg/kg of mice weight in 0.2 mL.
2. As the tumor reaches the diameter of 7 mm, immobilize the animal in immobilization chamber and inject 0.2 EBD in saline into the tail vein.
3. At each time point of evaluation, euthanize animals in CO_2 chamber for 2 min.
4. Place the animal ventrally and through midline incision, expose inferior vena cava, collect 0.2 mL of blood, and mix instantly with 2.8 mL of Isoton II, followed by centrifugation at 800 rpm for 5 min, then read by spectrophotometer at 620 nm.
5. After blood collection, cut the diaphragm and expose the heart, grasp the heart with tweezers, and using 20-mL syringe with 24-G needle, inject 20 mL of saline slowly into the left side of the heart to remove the dye from the blood component of any organ.
6. Expose the dorsal skin having the tumor, visually document the EBD color in the tumor tissue in contrast to surrounding skin using camera, remove the tumor from the base using surgical scissor, weigh, and add to 3 mL formamide.
7. Collect sample from other tissue similarly, weigh, and add to 3 mL formamide.
8. Incubate at 60°C water bath with shaking for 48 h to extract EBD.
9. Read by spectrophotometer at 620 nm and convert the reading into μg EBD/mg tissue using standard curve of EBD.

3.3. Preparing SMA-Micelles

1. Dissolve SMA powder in water at pH 5.0 at 10 mg/mL.
2. Dropwise add doxorubicin solution in DW at a concentration of 10 mg/mL.

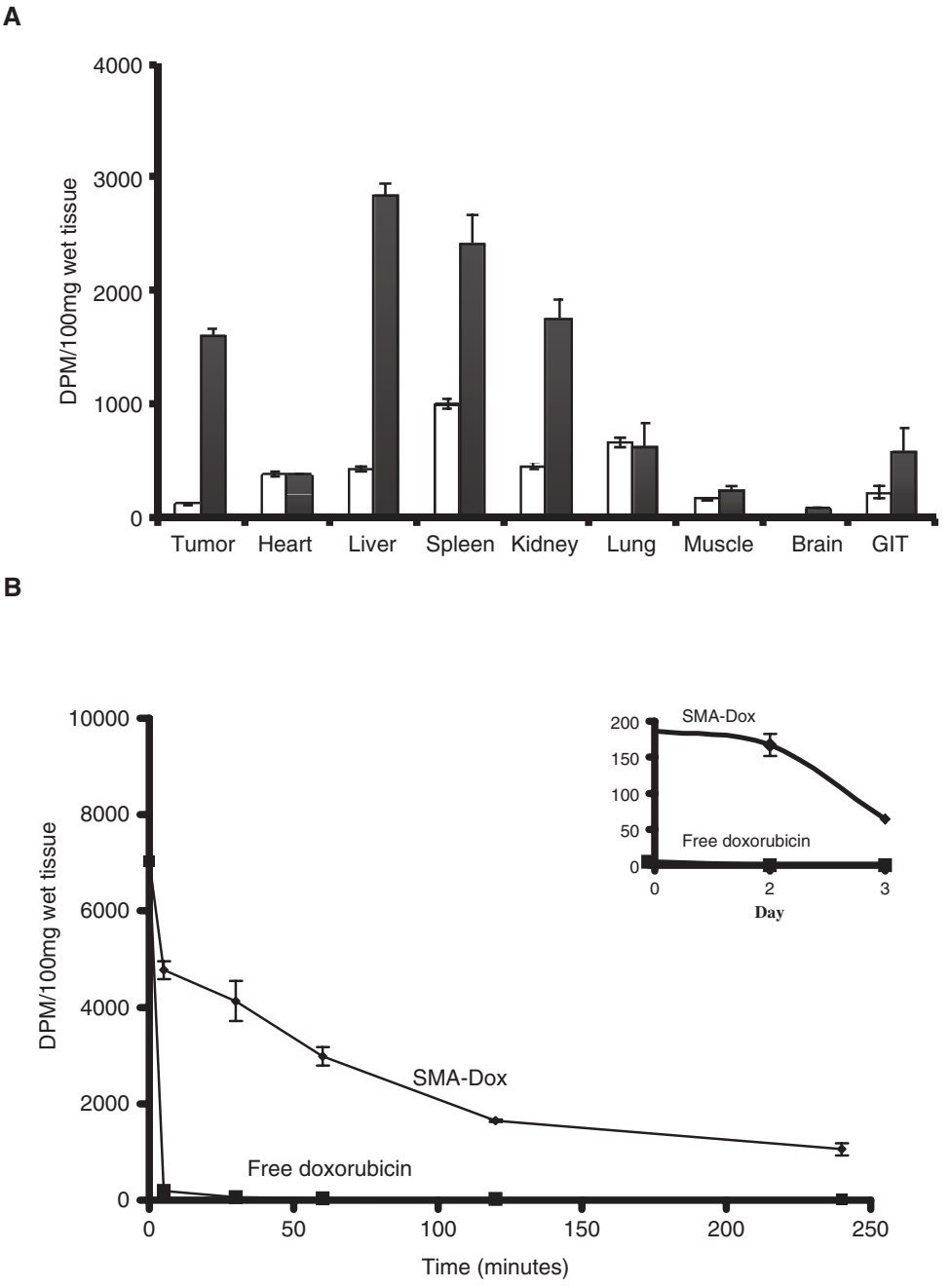

Fig. 3.6. (**a**) Micellar drug concentration in tumor was 13 times higher than free drug in animals 24 h after i.v. administration. (**b**) The $t^{1}/_{2}\,\alpha$ (half-life) of SMA-Dox micelles increased about 400-fold, while the area-under-concentration (AUC) time curve was 25 times greater than that of free drug when calculated for up to 3 days, the graph describes the result of method in **Section 3.4**. (Reproduced from 13 with permission from Elsevier.)

3. Add water soluble carbodiimide (EDAC) 10 mg/mL. The solution will precipitate.
4. Wash precipitates by centrifugation at 8,000 rpm for 5 min twice, and then reconstitute in pH 7, leave for 60 min to totally solubilize the micelles.
5. Wash and concentrate the micelle to one-tenth of the original volume by ultrafiltration with the Amicon ultrafiltration, repeat three times.
6. Measure concentration of the resulting micelle through UV, comparing it to standard curve of the absorbance of free doxorubicin.

3.4. Pharmacokinetics and Drug Distribution

1. Use animal model as described in **Section 3.1**.
2. Divide animals into two groups, control the group to receive radio-labeled free doxorubicin, and test the group to receive radio-labeled SMA-Dox micelles. Inject 5 mg/kg of doxorubicin equivalent through the tail vein in a 0.2-mL volume saline.
3. At scheduled time points, euthanize mice in CO_2 and collect blood samples from the inferior vena cava as in Step 4 of **Section 3.2**.
4. Inject 20 mL of saline to remove blood components from the blood vessels in the tissues as in Step 5 of **Section 3.2**, then collect and weigh tumor tissues, liver, kidney, gastrointestinal tract (GIT), heart, lung, brain, and muscles.
5. Mix each 100 mg sample of tissue with 1 mL of Soluene-350, solubilize the mixtures by incubation at 60°C for 4 h, after which add to 10 mL of Hionic Fluor LSC cocktail.
6. Measure the radioactivity of plasma and various tissues by using a beta liquid scintillation counter (**Fig. 3.6**).

4. Notes

1. Both xenogeneic and syngeneic animal models can be used; syngeneic model is preferred as it ensures natural tumor vessels development accounting for role of immunomodulators secreted by infiltrating neutrophils and macrophages on the tumor vasculature (22, 23).
2. Cancer cells should be passaged in animals twice before starting the final experiment.
3. Cell number needed to establish tumor in animals can vary from one tumor cell line to the other, usually ranges from 1 to 5 million cell per injection site.

4. Number of animal per experiment is chosen according to the time points, many points needed to be selected to reflect both the pharmacokinetics of free drug and the nano-sized drug (5, 30,120, 480, 720 min, and 1–2 days) are example of the time points that can be used.
5. Tumor size of 5–7 mm in diameter (7–10) must be used; larger tumor size tends to have poor vascularization as tumor necrosis develops centrally with collapse of the fragile tumor vasculature (**Fig. 3.1B, D**). Animals having under- or over-grown tumors should be removed.
6. Metastatic models can be used, however, metastatic tumor tends to show poor EPR effect due to its more deranged vessel development (24).
7. When injecting the tumor cells subcutaneously, avoid the hind limb of the animal as rapid growth of the tumor can affect animal mobility.
8. The use of SMA-micelles is experimental example; it can be substituted with any nano-sized drug of molecular weight above 40 kDa (**Fig. 3.1C**).
9. The injected dose calculation should be based on the active ingredient (cargo) dose, not on the total gram value of injected material including the polymer carrier.
10. Many macromolecular drug combine with plasma protein changing their in vivo molecular weight and biological properties, this phenomenon is species specific (25).
11. In the previous experimental examples, UV and radioactivity detection methods were used, in addition fluorescence properties could also be used. However, radioactivity detection is the most accurate and time efficient.
12. Ideal experiment should delineate the concentration of the carrier polymer from the drug cargo, double labeling of both the carrier polymer and the drug carrier can address this issue.
13. Expected gain of EPR effect is ~7- to 10-fold higher tumor concentration compared to free low molecular weight drug, combining passive EPR targeting with hypertension, ISDN, PDT, or ACE inhibitor can result in up to 30-fold higher tumor accumulation (26).
14. EPR effect is not limited to pharmacokinetics and biodistribution, the main benefit is more effective anticancer therapy with fewer side effects. In vivo anticancer assay and toxicity study complement the study of EPR effect.
15. EPR effect can also similarly be demonstrated in inflammatory tissue, however, less retention time is always observed compared to tumor tissues (11).

Acknowledgments

The author gratefully acknowledges the support of Prof. Hiroshi Maeda. The EPR effect was first described and extensively studied by Prof. Maeda's group. Techniques related to EPR effect, described in this chapter, were developed by Maeda's group in the Department of Microbiology, Kumamoto University, Japan.

References

1. Folkman, J. (1971) Tumor angiogenesis: therapeutic implications. *N Engl J Med* **285**, 1182–1186.
2. Skinner, S. A., Tutton, P. J., and O'Brien, P. E. (1990) Microvascular architecture of experimental colon tumors in the rat. *Cancer Res* **50**, 2411–2417.
3. Yuan, F., Salehi, H. A., Boucher, Y., Vasthare, U. S., Tuma, R. F., and Jain, R. K. (1994) Vascular permeability and microcirculation of gliomas and mammary carcinomas transplanted in rat and mouse cranial windows. *Cancer Res* **54**, 4564–4568.
4. Folkman, J. (1995) Angiogenesis in cancer, vascular, rheumatoid and other disease. *Nat Med* **1**, 27–31.
5. Hashizume, H., Baluk, P., Morikawa, S., McLean, J. W., Thurston, G., Roberge, S., Jain, R. K., and McDonald, D. M. (2000) Openings between defective endothelial cells explain tumor vessel leakiness. *Am J Pathol* **156**, 1363–1380.
6. Noguchi, Y., Wu, J., Duncan, R., Strohalm, J., Ulbrich, K., Akaike, T., and Maeda, H. (1998) Early phase tumor accumulation of macromolecules: a great difference in clearance rate between tumor and normal tissues. *Jpn J Cancer Res* **89**, 307–314.
7. Wu, J., Akaike, T., and Maeda, H. (1998) Modulation of enhanced vascular permeability in tumors by a bradykinin antagonist, a cyclooxygenase inhibitor, and a nitric oxide scavenger. *Cancer Res* **58**, 159–165.
8. Maeda, H., Akaike, T., Wu, J., Noguchi, Y., and Sakata, Y. (1996) Bradykinin and nitric oxide in infectious disease and cancer. *Immunopharmacology* **33**, 222–230.
9. Maeda, H., Matsumura, Y., and Kato, H. (1988) Purification and identification of [hydroxyprolyl3]bradykinin in ascitic fluid from a patient with gastric cancer. *J Biol Chem* **263**, 16051–16054.
10. Doi, K., Akaike, T., Horie, H., Noguchi, Y., Fujii, S., Beppu, T., Ogawa, M., and Maeda, H. (1996) Excessive production of nitric oxide in rat solid tumor and its implication in rapid tumor growth. *Cancer* **77**, 1598–1604.
11. Matsumura, Y. and Maeda, H. (1986) A new concept for macromolecular therapeutics in cancer chemotherapy: mechanism of tumoritropic accumulation of proteins and the antitumor agent smancs. *Cancer Res* **46**, 6387–6392.
12. Seymour, L. W., Miyamoto, Y., Maeda, H., Brereton, M., Strohalm, J., Ulbrich, K., and Duncan, R. (1995) Influence of molecular weight on passive tumour accumulation of a soluble macromolecular drug carrier. *Eur J Cancer* **31A**, 766–770.
13. Greish, K., Sawa, T., Fang, J., Akaike, T., and Maeda, H. (2004) SMA-doxorubicin, a new polymeric micellar drug for effective targeting to solid tumours. *J Control Release* **97**, 219–230.
14. Suzuki, M., Hori, K., Abe, I., Saito, S., and Sato, H. (1981) A new approach to cancer chemotherapy: selective enhancement of tumor blood flow with angiotensin II. *J Natl Cancer Inst* **67**, 663–669.
15. Li, C. J., Miyamoto, Y., Kojima, Y., and Maeda, H. (1993) Augmentation of tumour delivery of macromolecular drugs with reduced bone marrow delivery by elevating blood pressure. *Br J Cancer* **67**, 975–980.
16. Greish, K., Fang, J., Inutsuka, T., Nagamitsu, A., and Maeda, H. (2003) Macromolecular therapeutics: advantages and prospects with special emphasis on solid tumour targeting. *Clin Pharmacokinet* **42**, 1089–1105.
17. Tanaka, S., Akaike, T., Wu, J., Fang, J., Sawa, T., Ogawa, M., Beppu, T., and Maeda, H. (2003) Modulation of tumor-selective vascular blood flow and extravasation by the stable prostaglandin 12 analogue beraprost sodium. *J Drug Target* **11**, 45–52.
18. Meyer, R. E., Shan, S., DeAngelo, J., Dodge, R. K., Bonaventura, J., Ong, E. T., and Dewhirst, M. W. (1995) Nitric oxide synthase inhibition irreversibly decreases

perfusion in the R3230Ac rat mammary adenocarcinoma. *Br J Cancer* **71**, 1169–1174.
19. Okamoto, T., Akaike, T., Sawa, T., Miyamoto, Y., van der Vliet, A., and Maeda, H. (2001) Activation of matrix metalloproteinases by peroxynitrite-induced protein S-glutathiolation via disulfide S-oxide formation. *J Biol Chem* **276**, 29596–29602.
20. Dougherty, T. J., Gomer, C. J., Henderson, B. W., Jori, G., Kessel, D., Korbelik, M., Moan, J., and Peng, Q. (1998) Photodynamic therapy. *J Natl Cancer Inst* **90**, 889–905.
21. Chen, B., Pogue, B. W., Luna, J. M., Hardman, R. L., Hoopes, P. J., and Hasan, T. (2006) Tumor vascular permeabilization by vascular-targeting photosensitization: effects, mechanism, and therapeutic implications. *Clin Cancer Res* **12**, 917–923.
22. Nozawa, H., Chiu, C., and Hanahan, D. (2008) Infiltrating neutrophils mediate the initial angiogenic switch in a mouse model of multistage carcinogenesis. *Proc Natl Acad Sci USA* **33**, 12493–12498.
23. Furuya, M. and Yonemitsu, Y. (2008) Cancer neovascularization and proinflammatory microenvironments. *Curr Cancer Drug Targets* **4**, 253–265.
24. Nagamitsu, A., Inuzuka, T., Greish, K., and Maeda, H. (2007) SMANCS Dynamic therapy for various advanced solid tumors and promising clinical effects enhanced drug delivery by hydrodynamic modulation with vascular mediators, particularly angiotensin II, during arterial infusion. *DDS* **22**, 510–522.
25. Pahlman, I. and Gozzi, P. (1999) Serum protein binding of tolterodine and its major metabolites in humans and several animal species. *Biopharm Drug Dispos* **2**, 91–99.
26. Iyer, A. K., Khaled, G., Fang, J., and Maeda, H. (2006) Exploiting the enhanced permeability and retention effect for tumor targeting. *Drug Discov Today* **11**, 812–818.
27. Greish, K., Arun, I., Fang, J., and Maeda, H. (2006) Enhanced permeability and retention (EPR) effect and tumor-selective delivery of anticancer drugs. In *Delivery of Protein and Peptide Drugs in Cancer*. V. P. Torchilin(Ed.), Imperial College Press, London, 37–52.